Vol. 06, No. 1 (2024) 171-178, doi: 10.24874/PES06.01.019

Proceedings on Engineering Sciences

www.pesjournal.net

EXPERIMENTAL STUDY OF SHALLOW FOUNDATION SETTLEMENT UNDER DYNAMIC LOAD IN REINFORCED SANDY SOIL

Naser Abed Hasen[1]
Jawdat K. Abbas

Received 04.03.2023.
Received in revised form 25.07.2023.
Accepted 01.08.2023.
UDC – 551.244

Keywords:

Settlement, Dynamic load, Geogrid, Sandy soil, Settlement

A B S T R A C T

*This research studies geogrid reinforcement of sandy soils under the influence of the three earthquakes (Halabjah, Bolunun, and Ali Al-Gharbi) due to the recent increase in seismic activity and the need to reduce damage to foundations due to settlement. Sand samples prepared with a relative density of 70%, with and without geogrid reinforcement, were tested on a shaking (vibrating table) table. Five geogrid layers were used, respectively. Settlement occurs due to dynamic force, and the plastic foundation was used with dimensions of 100 * 100 * 30 mm. Withstands a static load of 5.294 kN/m2. Increasing the acceleration of the earthquake leads to an increase in the settlement of the foundation in the sandy soil. The greater the number of geogrids reinforcing layers, the leads to a decrease in the base settlement, where the rate of settlement decrease is greater, the lower the earthquake acceleration and the greater the number of geogrid reinforcement layers. The time of onset of settlement and the general pattern of settlement are similar in all cases studied. The rate of settlement is approximately twice as high when the soil is saturated than when the soil is dry, and the effect of geogrids is less for the soil when it is saturated than when it is dry.*

1. INTRODUCTION

Soil reinforcement is not a new science but has a lengthy history. French architect and engineer Henri Vidal were the first to use systemic soil reinforcement in modern society. Binquet and Lee (1975), developed research with planar aluminum strips, providing the groundwork for systematic investigation. Metal reinforcement in a planar shape, which can be costly and corrosive, was often utilized. On the other hand, the development of polymeric geosynthetics has resulted in a soil-reinforcing renaissance. Geogrid is one of the newest geosynthetic reinforcers that has been explored extensively. The current study demonstrated the effect of geogrid-enhanced earth on the transfer of dynamic loads under the foundations. The assessment was carried out, focusing mainly on the surface settlement behavior of the foundations.

The devastating results that occur as a result of the descent prompt many researchers to study, investigate, analyze and predict the behavior of soil and foundation during earthquakes to avoid or reduce these effects. Developed studies and research have been followed and relied on methods, theories and hypotheses to simulate the failure mechanism. Some of these methods are numerical, empirical and numerical empirical as they depend on parameters of the nature, condition and

[1] Corresponding author: Naser Abed Hasen
Email: Naser.a.hassan@tu.edu.iq

movement of the soil, where they analyzed the characteristics of the soil and its field condition as a factor controlling its behavior during the earthquake.

2. PREVIOUS STUDIES ON SEISMIC SETTLEMENT DETERMINATION

Das et al. (1995) Saturated clay reinforced with geogrid and loaded cyclically low-frequency varied. Before applying cyclic loads, the surface section foundation's permanent settlement strip footing was loaded appropriately. Change frequency and cycle loading amplitude. Geogrid reinforcement reduced permanent settlement 20%-30%. Puri and Prakash (2007) Investigated seismically loaded shallow foundations and piles in liquefied and non-liquefied soils. An experimental approach that correlated earthquake acceleration, frequency, dynamic bearing capacity factors (Nc, Nq, Nγ), and structure aspects ratio evaluated shallow footing bearing capacity loss and forecasted settlement increases. Tafreshi and Dawson (2010) Studied flat, three-dimensional reinforced sand strip foundations. Loading continued until foundations settled. Repeated loading develops a baseline maximum settlement that is substantially better than unreinforced sand and comparable to planar or three-dimensionally reinforced sandy soil. Sand reinforcement lowered foundation settlement. Sawwaf and Nazir (2012) After modifying a fraction of the concentrated sandy soil layer and reinforcing the structural floor, a strip foundation was tested on a slope of loose sand under periodic and cyclical pressures. the reinforced and regenerated sand is periodically cemented and this results in a reduced foundation settlement. Puri and Prakash (2013) calculated seismic-induced soil shear stress. If volume loading is constant, shear stress is equal to volumetric stress. They found that earthquake-induced soil volume change plus building pressure equals total settlement. It's official. Hotti et al. (2014) studied the behavior of a square foundation based on sandy soil reinforced with geogrids under load and no-load conditions. The results showed that using the geogrid reduces the settlement amount. Boushehrian and Afzali (2016) The anchor grid technique reduced soil settlement by 54% upon dynamic load shedding as the researchers used reinforcement to stabilize and alter the behavior of shallow foundations. Al-Salakh and Albusoda (2020) The research establishment studied footing sinking on liquefied soil using experimental and theoretical methods on the shallow footing on sandy soils at earthquake loads vary. And the adjusted equation demonstrated a significant level of convergence with the measured settlement values. Karim *et al.* (2020) studied settlement and lateral displacement of shallow foundations on saturated sandy soils reinforced and unreinforced with geogrids under variable frequency and amplitude loading. They found that the reinforcing material prevents settlement. Alireza (2021) Geogrid soil strengthening reduced periodic stress-induced sandy slope strip foundation settlement. More loading and unloading cycles and cyclic loading capacity during geogrid reinforcement improved permanent settlement.

3. LABORATORY WORK

3.1 Soil used

In the standard tests, sand from Tikrit was used as the soil. The sand has already been air-dried, crushed, and sieved through a No. 4 (2 mm) sieve. Its 70% sand density was evaluated in a variety of ways. When performing soil tests, BS and ASTM requirements are followed. Figure represents the grain size distribution and the results of a sieve analysis test on used sand. Table 1 summarizes the characteristic features found during tests on sand and clay that use the approved method.

Table 1. Physical and chemical properties and tests carried out on soils with the used standard

Soil Property	DenseSand	Standard
Relative density, D_r (%)	70	-
Maximum dry unit weight, $\gamma_{d\,max}$ (KN/m³)	17.32	ASTM D4253 (2000)
Minimum dry unit weight, $\gamma_{d\,min}$ (KN/m³)	14.48	ASTM D4254 (2000)
Specific gravity, G_s	2.647	ASTM D854 (2014)
Maximum void ratio, e_{max}	0.793	-
Minimum void ratio, e_{min}	0.499	-
D_{10}, D_{30}, D_{50}, D_{60} (mm)	0.152, 0.285, 0.328, 0.41	ASTM D422 (2007)
Coefficient of uniformity, C_u	2.697	
Coefficient of curvature, C_c	1.303	
Soil classification (USCS) Unified Soil Classification System	(SP)	ASTM D2487 (2010)
Friction angle, φ	37.48°	ASTM D4767 (2011)

3.2 Geogrid reinforcement

This study utilizes a single type of geogrid. The TX140 triaxial A geogrid is made from a punched polypropylene sheet and orientated in three roughly equal directions, resulting in ribs having a high degree of macromolecular chains. This path extends at least partially through the integral node's mass. Figure 1 shows the geogrid's structure, and Table 2 explains the parameters that influence the performance of a mechanically stabilized layer. Earlier research determined the depth of the first layer, U/B = 0.3, and the depth of the remaining layers, h/B = 0.4. Based on past results, the researchers selected (N = 5) layers of reinforcement. The ideal ratio of the vertical distance between layers (h/B = 0.5) and the relative efficiency of the vertical distance between layers (u/B = 0.35-0.45) are both equal to 0.5, according to Al-Tirkity and Al-Taay (2012).

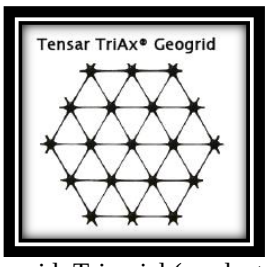

Figure 1. Geo-grid: Tri-axial (product specification)

Table 2. Geogrid properties (product specification)

Index Properties	Longitudinal/ Transverse	Diagonal	General
Rib pitch (2), mm (in)	40 (1.60)	40 (1.60)	
Mid-rib depth (2), mm (in)	1.2 (0.05)	1.2 (0.05)	
Mid-rib width (2), mm (in)	1.1 (0.04)	1.1 (0.04)	
Rib shape			Rectangular
Aperture shape			Triangular
Structural Integrity			
Junction efficiency%			93
sotropic Stiffness Ratio			0.6
Radial stiffness at low strain, kN/m @ 0.5% strain (lb/ft @ 0.5% strain)			225 (15,430)
Durability			
Resistance to chemical degradation			100%
Resistance to ultra-violet light and weathering			100%

4. SETUP DESIGN AND MANUFACTURING OF SHAKE TABLE EXPERIMENTAL STUDY

4.1 Mechanical components of a shake table:

Al-Sammaraey (2018) The experiment required a vibration table with a 60*120*10 cm steel structure attached to the ground and an 80*80*8 cm cart base. Steel tubes with wheels move the cart's bottom. 10mm rubber supported the outside frame. The rubber pad is flush with the floor and vibration-free. Plate 1 demonstrates how a 40-mm ball screw shaft turns the motor's rotational motion into linear displacement. The rocking table frame has two ball screw nut brackets. One bracket and the rocking table frame held the drive rod. Allows ball screw movement across the frame.

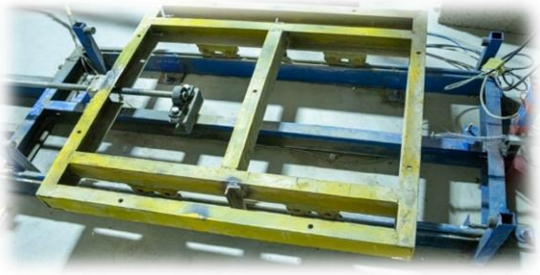

Plate 1. Shaking table mechanical parts

4.2 Servo Motor and Drive

Servomotors are efficient and accurately control angular position, direction, and velocity. Position sensor generators drive it. A position indexer control module (movement tasks) was easily interfaced with a Kollmorgen servo motor "AKM 73P-ACCNDA01" with model number "AKD-P02407-NBEC-0000," three-phase power supply, and EtherCAT protocol connection. Table 3 lists product specs, whereas Plate 2 shows the servo motor and drive. Figure 2 shows the Arduino setup. Arduino uses computer seismic data. The inverter matches the shaker table's input wave, moving the car.

Table 3. Servo motor specifications

AKM Servo motor	Servo Drive	Frame Size (NEMA"/mm)	Torque (N.m)	Rated Speed RPM	Power Prtd (watts)	Inertia (JM)	Feedback Device	Device Resolution (Cycles or Line/rev)
AKM73P	AKD-P02407	na/180	41.4	2400	7130	92.1	Endat 2.1 (DA)	2048

a. Servo motor b. Servo motor drive

.**Plate 2.** Servo motor and servo motor drive

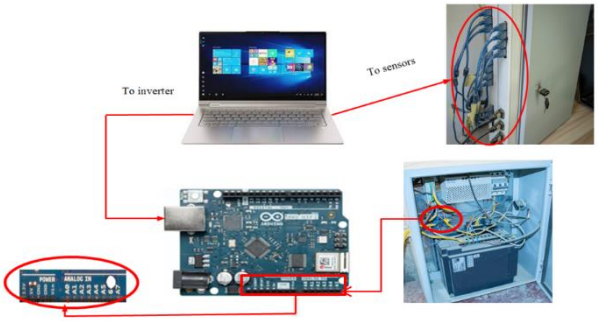

Figure 2. Arduino Export Data to Inverter

5. INSTRUMENTATIONS

5.1 LVDT Sensor

The linear variable differential inductor estimated direct displacement (LVDT). A sealed circuit that works in wet and dusty environments and a standard output signal make the DC LVDT great. A computer with a stainless-steel casing and a 20-millimeter hydraulic cylinder. Valve detection, location, and control. Plate 3 shows the 100mm LVDTs used in this study. LVDT is installed on a foundation on top for measuring settlement.

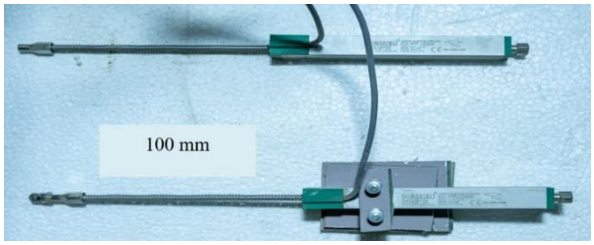

Plate 3. LVDT Sensors

6. IMPLEMENTATION EARTHQUAKE DATA

The Center for Engineering Strong Motion Data (CESMD), which works with the US Geological Survey (USGS) and the California Geological Survey (CGS)) (131), and the Iraqi Meteorological Organization and Seismology provided the data utilized as natural seismic activity. Three different earthquakes depicted and applied natural acceleration views for Halabjah, Ali Al-Gharbi, and Bolunun to determine whether or not acceleration characteristics influenced foundation settlement possibility. Tables 4 show the studied cases of acceleration history.

Table 4. Information of earthquake data.

Earthquake	Halabjah	Ali Al-Gharbi	Bolunun
Region:	Iraq-Iran border	Iraq	Turkey
Date (UTC*):	2017-11-12 18:18:17	2015-09-25 06:10:24	2000-02-14 06:56:36
Magnitude, (Mw):	7.3 Mw	4.9 M_L	5.0 Mw
Modified Mercalli Intensity, (MMI):	VIII- Moderated heavy	N/A	VIII
Epicenter depth, (km):	19.0	10.0	15.7
Shake duration, (sec):	300	160	354
Station distance to epicenter, (km):	218.8	106.9	168.7
Sampling frequency, (Hz):	10	10	12
Acceleration direction:	E-W	N-S	N-W
Maximum acceleration, (g):	0.161	0.101	0.13187
Station code:	BHD	IBDR	MET
Reference:	Iraqi Meteorological Organization and Seismology	Iraqi Meteorological Organization and Seismology	www.strongmotiomcenter.org

7. EARTHQUAKE SIMULATOR FOR PC

LabVIEW 2020 was used to develop the Earthquake Simulator. Software controls input shaking acceleration, shaking, DAQ, data logging, analysis, and reporting. Earthquake Simulator has a total of four stages.

7.1. Choose Input Shaking Acceleration

At this point, the g-unit input acceleration information can be developed, and the type, duration, and information period can be chosen. Data periods can vary. These formats contain acceleration data: Use Halabjah, Bolunun, and Ali Al-Gharbi earthquake acceleration histories. Plate 4 shows the library form selection process. The software analyzes acceleration data and converts it to velocity, displacement, and the maximum acceptable acceleration.

Plate 4. Choose earthquake from the library.

7.2 Data Logging, Shaking, and Data Acquisition (DAQ)

This step sets test data, soil profile, and foundation qualities. Sensor testing follows. The table shakes as the test begins. Sensor data is shown in real-time as soil accelerometers monitor settlement. Plate 5 shows shaking and DAQ. After the test, record and transfer the data to preserve it.

a. Test information b. Data logging

Plate 5. Test information of shaking and DAQ and Data logging

7.3 Analysis and reporting of data

At this stage, the outcome data is analyzed and presented. Where the data was exported as just an Excel spreadsheet. Plate 6 shows the stage of data analysis and reporting.

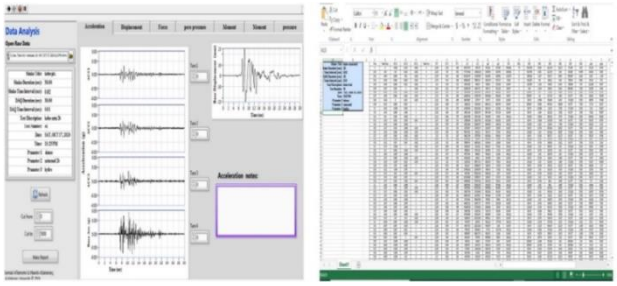

a. Data analysis b. Microsoft excel report

Plate 6. Data analysis and reporting.

8. FLEXIBLE LAMINAR SHEAR BOX (FLSB)

Bhattacharya et al., (2012) Various containers, their advantages and disadvantages, and model container needs were discussed. Flexible laminar containers were chosen to reduce wave reflections from the rigid border and end wall lateral stiffness. The soil might continue to control the soil-box system. The FLSB contains tested foundation and soil models. This box reduces boundaries in fixed-side boxes. Due to laminae horizontal deformation, the boundary is lower than when simulating soil behavior, such as reflectance from the side. FLSB end walls match the soil model's shear stiffness. 12 square steel laminae are placed on top and connected to tracks that enable the FLSB to slide in one direction. Figures 3 show laminae steel tube dimensions. It is welded as a square frame (600*600 inside and 700*700 outside) with a total height of 600 mm and 50 mm for each lamina. Thin ball-bearing

linear rail strips were welded between each lamina. 500 mm long, 43 mm wide, and 12.5 mm high, these strips. The FLSB was 720 mm tall after the laminae were joined to a steel square plate base frame with an outside dimension of (800*800) mm and a height of 120 mm. The pushing strength was divided by the usual force of the laminae weight stacked on top.

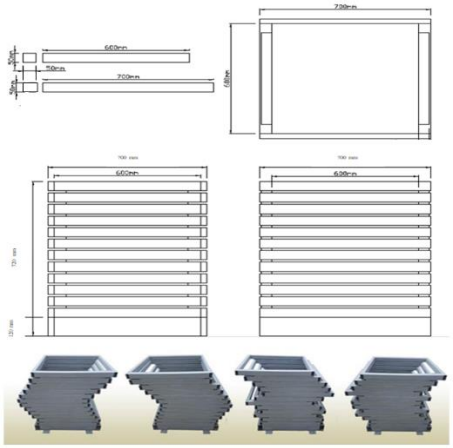

Figure 3. Flexible laminar shear box and its dimensions

9. SATURATED SYSTEM

To saturate the soil model, a water distribution panel with 0.5-inch (12.7 mm) diameter pipes constructed a square pipes network and was cloth-encased to prevent clogging. The saturation system, depicted in plate 7, was placed on the base of the laminar box behind a 120-mm-thick coarse grain filter to prevent the soil from dragging with water when a water pump drained it after the test.

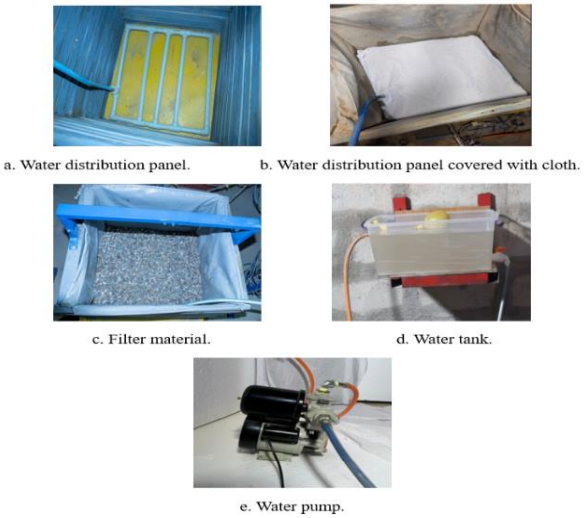

a. Water distribution panel. b. Water distribution panel covered with cloth.

c. Filter material. d. Water tank.

e. Water pump.

Plate 7. Soil saturation system

10. FOOTING MODEL

The experimental work shown plate 8 used a foundation made from a solid plastic block 100 mm x 100 mm x 30 mm, which is similar to the full-size model (1500 mm x 1500 mm x 450 mm). Sandpaper was placed on the block's bottom and weighed 5.4 kg to simulate the friction angle of saturated loose sand with plastic.

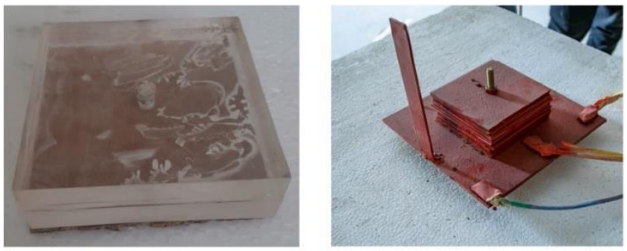

a. footing b. footing with load

Plate 8. footing model

11. PROGRAM FOR SHAKE TABLE TESTING

36 shaking table tests on sand density, layered subsoil, dry soil, and saturation soil were performed, along with a range of earthquake acceleration histories. Figures 4 show the testing program flowchart.

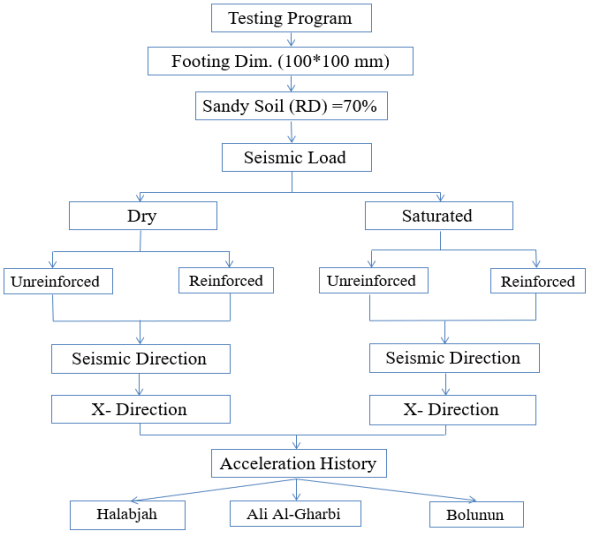

Figure 4. the testing program

12. GEOGRID REINFORCEMENT'S EFFECT ON SURFACE SETTLEMENT UNDER DYNAMIC LOAD:

This study examines whether geogrid-reinforced soil transmits dynamic loads beneath foundations. Surface settlement behavior was essential to evaluation. Moving earthquakes and geogrid reinforcing layers will also be examined. Reinforcing the geogrid network reduces the maximum cycle load intensity. The Permanent Settlement decreases the Settlement by 20–30% compared to the unreinforced version, Das et al. (1995).

The settlement resulting from the three earthquakes (Halabjah, Bolunun, and Ali al-Gharbi) was studied for foundations based on dry and saturated sandy soils and

their strengthening using geogrid layers. The results are in Tables 5 to 10 and figure 5 to 10. When observing the effect of the Halabjah earthquake on the settlement of the foundation based on dry sandy soil in Table 5 and Figure 5, notice that the settlement reaches nearly half of D_f (the high of the foundation) in unconsolidated soils. The rate of decrease begins with the settlement, and the reduction increases gradually as the number of reinforcing layers increases.

When observing the effect of the Halabjah earthquake on the settlement of the foundation based on the saturated sandy soil in Table 5 and Figure 6, note that the settlement reaches the full depth of the foundation in the non-reinforced soil. The rate of decrease begins with the settlement, and the rate of decline increases gradually with the increase in the number of reinforcing layers.

Table 5. Footing settlement for the influence of the Halabjah earthquake on dry and saturated sandy soil

Case of soil	Settlement of dry sandy soil (mm)	Percentage decrease in the settlement in dry sandy soil	Settlement of saturated sandy soil (mm)	Percentage decrease in the settlement in saturated sandy soil
Unreinforced soil	$0.48D_f$	-	$1.03D_f$	-
1 Layer of geogrid	$0.44D_f$	7%	$1D_f$	3%
2 Layers of geogrid	$0.42D_f$	12%	$0.93D_f$	6.67%
3 Layers of geogrid	$0.38D_f$	18.8%	$0.91D_f$	11.65%
4 Layers of geogrid	$0.34D_f$	27.2%	$0.86D_f$	19.49%
5 Layers of geogrid	$0.29D_f$	37.3%	$0.8D_f$	22%

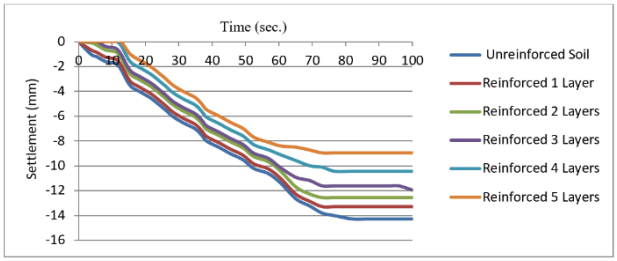

Figure 5. Settlement of Foundation with Halabjah Earthquake in Dry Sand

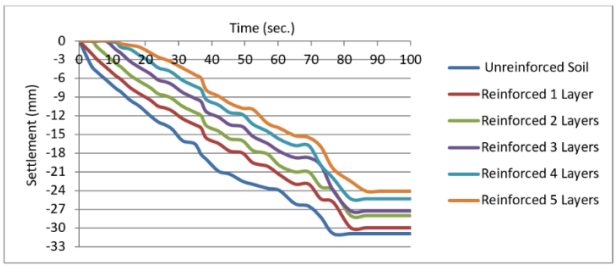

Figure 6. Settlement of Foundation with Halabjah Earthquake in Saturated Sand

When studying the results related to the Bolunun earthquake effect on the foundation's settlement based on dry sandy soil in Table 6 and Figure 7, notice that the settlement reaches approximately $0.46D_f$ in unreinforced soils. The rate of decrease begins with the settlement, and the percentage of decrease increases gradually with the increase in the number of reinforcing layers.

When studying the results related to the effect of the Bolunun earthquake on the settlement of the foundation based on the saturated sandy soil in Table 6 and Figure 8, note that the settlement reaches $0.99D_f$ in the unconsolidated soil. The rate of decrease begins with settlement, and the rate of decrease increases gradually as the number of reinforcing layers increases.

Table 6. Footing settlement for the influence of the Bolunun earthquake on dry and saturated sandy soil

Case of soil	Settlement of dry sandy soil (mm)	Percentage decrease in the settlement in dry sandy soil	Settlement of saturated sandy soil (mm)	Percentage decrease in the settlement in saturated sandy soil
Unreinforced soil	$0.46D_f$	-	$0.99D_f$	-
1 Layer of geogrid	$0.42D_f$	8.7%	$0.93D_f$	5.72%
2 Layers of geogrid	$0.39D_f$	14.5%	$0.87D_f$	11.78%
3 Layers of geogrid	$0.36D_f$	21.36%	$0.84D_f$	15.15%
4 Layers of geogrid	$0.32D_f$	29%	$0.77D_f$	21.88%
5 Layers of geogrid	$0.28D_f$	38.45%	$0.71D_f$	27.6%

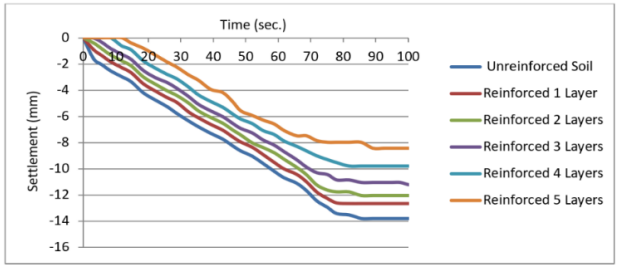

Figure 7. Settlement of Foundation with Bolunun Earthquake in Dry Sand

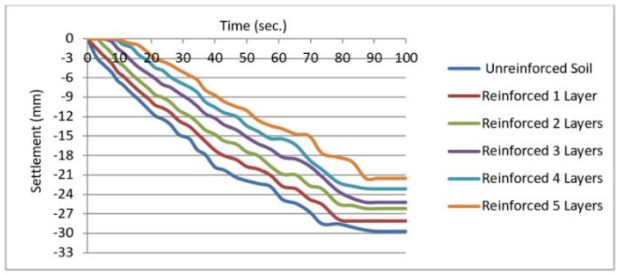

Figure 8. Settlement of Foundation with Bolunun Earthquake in Saturated Sand

When studying the results of the Ali Al-Gharbi earthquack impact on the foundation's settlement based on dry sandy soil in Table 7 and Figure 9, note that the settlement reaches approximately $0.42D_f$ in unreinforced soils. The rate of decrease begins with the settlement, and the percentage of decrease increases gradually with the increase in the number of reinforcing layers.

When studying the impact of the Ali Al-Gharbi tremor on the settlement of the foundation based on the saturated sandy soil in Table 7 and Figure 10, note that the settlement reaches $0.95D_f$ in the unconsolidated soil. The rate of decrease begins with settlement, and the rate of decrease increases gradually as the number of reinforcing layers increases.

Table 7. Footing settlement for the influence of the Ali Al-Gharbi earthquake on dry and saturated sandy soil

Case of soil	Settlement of dry sandy soil (mm)	Percentage decrease in the settlement in dry sandy soil	Settlement of saturated sandy soil (mm)	Percentage decrease in the settlement in saturated sandy soil
Unreinforced soil	$0.42D_f$	-	$0.95D_f$	-
1 Layer of geogrid	$0.4D_f$	5.21%	$0.89D_f$	5.61%
2 Layers of geogrid	$0.38D_f$	8.76%	$0.81D_f$	14.56%
3 Layers of geogrid	$0.33D_f$	20.22%	$0.77D_f$	18.94%
4 Layers of geogrid	$0.28D_f$	31.67%	$0.7D_f$	26.31%
5 Layers of geogrid	$0.24D_f$	41.54%	$0.63D_f$	30.52%

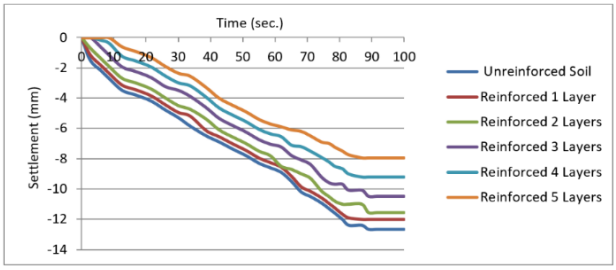

Figure 9. Settlement of Foundation with Ali Al-Garbi Earthquake in Dry Sand

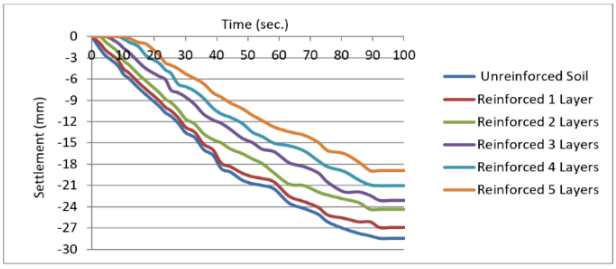

Figure 10. Settlement of Foundation with Ali Al-Garbi Earthquake in Saturated Sand

Figures 5, 7, and 9 show the effects of earthquakes (Halabjah, Polunun, and Ali Al-Gharbi) on the settlement of a foundation based on dry sandy soil unreinforced and reinforced with layers of geogrids. For unreinforced sandy soils, the rate of settlement is related to the high of the foundation D_f, which increases as the earthquake's acceleration increases. It has been thoroughly discussed at the top. Concerning the decrease in the rate of settlement in comparison to the number of layers for the three earthquakes and observed that the lower the acceleration of the earthquake, the greater the rate of decrease of the settlement, as the earthquake with the most significant rate of decrease in the settlement, was the Ali Al-Gharbi earthquake, and also related to the initial timing of the start of the settlement, it is close to the three earthquakes. Noticed a close earthquake after the final time of settlement.

Figures 6, 8, and 10 show the effect of the acceleration of three earthquakes (Halabjah, Polunun, and Ali al-Gharbi) on the settlement of unreinforced sandy soil armed with geogrid, respectively and seen that the descent to the foundations is remarkably rapid. It is essential because it completely submerges the foundation in the event of the Halabjah earthquake for the saturation soil that has been unreinforced and reinforced with a single layer of geogrid, as well as for the other earthquakes. The rate of descent about the high of the foundation D_f is large, and observe that the less the acceleration of the earthquake, the greater the rate of decrease of the settlement, as the earthquake that had the most significant rate of decrease in the settlement, and also about the initial timing of the start of the settlement, it is close to the three earthquakes, noticed a close earthquake after the final time of settlement.

13. CONCLUSION

The experimental technique adopted in this study with the aim Simulation, representation and evaluation of the descent of shallow foundations under the influence of earthquakes in dry and wet sandy soil conditions in the unreinforced and strengthened state to be suitable and give accurate and consistent results under seismic load conditions. Geogrid reinforcement system has been found to be effective in reducing the effect of foundation settlement. The following results were obtained:

1. In dry, saturated sandy soils, the settlement increases when the acceleration of the earthquake increase.
2. The higher the number of geogrid reinforcing layers, the lower the settlement of the foundation.
3. The less the acceleration of the earthquake and the greater the number of geogrid reinforcement layers, the greater the rate of decrease in settlement.
4. The initial timing at which the settlement takes place is close to all the studied cases, and the general behavior of the settlement is near.
5. The settlement rate in saturated soil is almost equal to two times the settlement of dry soil, and the decrease in settlement for saturated soil is less than that of dry soil.

References:

Al-Salakh, A. M., & Albusoda, B. S. (2020). Experimental and theoretical determination of settlement of shallow footing on liquefiable soil. *Journal of Engineering*, *26*(9), 155-164..

Al-Sammaraey, M. M. A. (2018). Experimental and Numerical Liquefaction Analysis of Layered Sand Soil under Shallow Spread Footing (Doctoral dissertation, Department of Civil Engineering, Al-Nahrain University).

Al-Tirkity, J. K., & Al-Taay, A. H. (2012). Bearing capacity of eccentrically loaded strip footing on geogrid reinforced sand. *Tikrit Journal of Engineering Sciences*, *19*(1), 14-22.

Bhattacharya, S., Lombardi, D., Dihoru, L., Dietz, M. S., Crewe, A. J., & Taylor, C. A. (2012). Model container design for soil-structure interaction studies. In *Role of seismic testing facilities in performance-based earthquake engineering: SERIES workshop* (pp. 135-158). Springer Netherlands.

Binquet, J., & Lee, K. L. (1975). Bearing capacity tests on reinforced earth slabs. *Journal of the geotechnical Engineering Division*, *101*(12), 1241-1255.

Boushehrian, A. H. (2021). Reinforcement Effects on The Permanent Settlement of Sandy Slopes Under Cyclic Loading. *AUT Journal of Civil Engineering*, *5*(3), 3-3.

Boushehrian, A. H., & Afzali, A. (2016). Experimental investigation of dynamic behavior of shallow foundation resting on the reinforced sand with embedded pipes. *International Journal of Geography and Geology*, *5*(9), 182-193.

Das, B. M., Shin, E. C., Shin, B. W., Lee, B. J., & Jung, K. T. (1995). Dynamic Loading Induced Settlement of Strip Foundation on Geogrid-Reinforced Clay. *Third International Conference on Recent Advances in Geotechnical Earthquake Engineering & Soil Dynamics*, 3, 2.29.

El Sawwaf, M. A., & Nazir, A. K. (2012). Cyclic settlement behavior of strip footings resting on reinforced layered sand slope. *Journal of Advanced research*, *3*(4), 315-324.

Hotti, B., Rakaraddi, P. G., & Kodde, S. (2014). Behavior of square footing resting on reinforced sand subjected to incremental loading and unloading. *International Journal of Research in Engineering and Technology*, *3*(6).

Karim, H. H., Samueel, Z. W., & Hussein, M. A. (2020, July). Investigation of the behavior of shallow machine foundation resting on a saturated layered sandy soil subjected to a dynamic load. *2nd International Conference on Civil and Environmental Engineering Technologies*, 888.

Puri, V. K., & Prakash, S. (2007). On Foundations Under Seismic Loads. *4th International Conference on Earthquake Geotechnical Engineering*, 1118, 25-28.

Puri, V. K., & Prakash, S. (2013). Shallow foundations for seismic loads: Design considerations. *Seventh International Conference on Case Histories in Geotechnical Engineering*, *27*(6), 497-505.

Tafreshi, S. M., & Dawson, A. R. (2010). Behaviour of footings on reinforced sand subjected to repeated loading–Comparing use of 3D and planar geotextile. *Geotextiles and Geomembranes*, *28*(5), 434-447.

Naser Abed Hasen
Civil Department, Engineering College,
Tikrit University, Tikrit, Iraq
Naser.a.hassan@tu.edu.iq

Jawdat K. Abbas
Civil Department, Engineering College,
Tikrit University, Tikrit, Iraq